



# A reliability-based approach to evaluating the stability of high rockfill dams using a nonlinear shear strength criterion



Z.Y. Wu, Y.L. Li\*, J.K. Chen, H. Zhang, L. Pei

State Key Laboratory of Hydraulics and Mountain River Engineering, Sichuan University, No. 24 South Section 1, Yihuan Road, Chengdu 610065, China  
College of Hydraulic and Hydroelectric Engineering, Sichuan University, No. 24 South Section 1, Yihuan Road, Chengdu 610065, China

## ARTICLE INFO

### Article history:

Received 8 May 2012  
Received in revised form 12 January 2013  
Accepted 12 January 2013  
Available online 5 March 2013

### Keywords:

Reliability  
Stability  
Rockfill dams  
Nonlinear shear strength criterion

## ABSTRACT

In recent years, many high rockfill dams have been constructed in China for the purpose of hydropower generation. One of the critical aspects of rockfill dam design is the analysis of slope stability. Triaxial compression tests show that the failure envelopes of rockfills are curved and that nonlinear shear strength criteria yield better predictions of the shear strengths of rockfills than the Mohr–Coulomb criterion. Because the determination of shear strength parameters involves uncertainties, a reliability-based methodology was developed for use in evaluating the failure probability of rockfill dam slopes by integrating Bishop's simplified method, Duncan's nonlinear strength criterion and the first-order second-moment reliability method presented in this paper. A computer program, SCU-SLIDE, was developed and its outputs validated by comparison with Monte Carlo simulation results. The approach developed was used to study the stability of the Shuang Jiang Kou rockfill embankment dam, which when completed will be the tallest dam in the world. The results of the stability analysis are discussed and conclusions are presented in this paper.

© 2013 Published by Elsevier Ltd.

## 1. Introduction

Many high rockfill dams are under construction in China, such as the Chang He Ba dam (240 m), the Nuo Za Du dam (261.5 m), the Liang He Kou dam (293 m), the Gu Shui dam (305 m) and the Shuang Jiang Kou dam (314 m). Slope stability analysis is a major component of the safety evaluation of rockfill dams. Two key issues in slope stability analysis are the shear strength criteria used for embankment materials and the computational methods used in the analysis.

Large-scale drained triaxial compression tests show that the friction angle of rockfill is not constant under different confining pressures, due to dilatancy and particle breakage. The friction angle can vary from approximately 55 degrees at very low normal pressures to approximately 35 degrees at very high normal pressures [1], and the failure envelopes exhibit pronounced curvature, particularly at low pressure levels [2].

The well-known Mohr–Coulomb criterion is based on fitting a straight line to the failure envelope. Both the cohesion and the friction angle are considered independent of the stress state. Because the friction angle of rockfill varies with the confining (normal) pressure, the failure envelope of rockfill is not linear. Thus, in the

case of rockfill, nonlinear shear criteria provide a better fit to triaxial test data than the Mohr–Coulomb criterion.

Moreover, if the cohesion of rockfill is assumed to be null (purely frictional) according to the Mohr–Coulomb criterion, at low normal stress levels, such as those at the outer face of a rockfill dam, the shear strength is quite low. In stability calculations, the slip surfaces of a rockfill surface would thus have safety factors lower than 1. That is, the rockfill surface would be unstable, which is not realistic. Nonlinear shear criteria assign higher shear strength parameters to superficial slip surfaces, which as a result do not have unrealistically low safety factors [3]. In short, evaluating the slope stability of rockfill dams (especially for high rockfill dams) with nonlinear shear criteria yields more accurate and more reasonable results [4].

Conventional deterministic analysis uses a safety factor in slope stability estimation. The safety factor is defined as the ratio of resisting forces to driving forces on a specific slip surface. A safety factor lower than 1 indicates that the slope is unstable. Due to uncertainties involved in determining the available strength of the soil, the selection of suitable values for the soil strength parameters and an allowable safety factor is difficult and is often based on engineering judgment and experience. Even so, the use of a single value for the safety factor would be misleading because a slope whose stability is calculated with a single safety factor value may in fact pose different risk levels, depending on the degree of variability of the strength parameters.

\* Corresponding author at: College of Hydraulic and Hydroelectric Engineering, Sichuan University, No. 24 South Section 1, Yihuan Road, Chengdu 610065, China.  
E-mail address: [liyanling\\_01@163.com](mailto:liyanling_01@163.com) (Y.L. Li).

The application of reliability theory to the analysis of the stability of slopes and embankments has been pursued over the last four decades. Some of the latest representative publications include Tang et al. [5], Zhang et al. [6], Zhang et al. [7], Raihan et al. [8], Chiu et al. [9], Irigaray et al. [10], Fisher and Eberhardt [11], Naghadehi et al. [12], Srivastava and Babu [13], Leynaud and Sultan [14], Suchomel and Masin [15], Wang et al. [16], Chowdhury et al. [17], and Mbarka et al. [18], among others. However, these studies have not addressed reliability analysis of the stability of rockfill embankments based on nonlinear shear criteria.

This paper proposes a reliability-based approach by which the uncertainties associated with the nonlinear strength parameters involved in slope stability analysis of high rockfill dams can be modeled and analyzed. The limit state function of slope stability is formulated using Bishop’s simplified method as the stability model. The shear strength of coarse-grained soils, such as rockfill, is determined using Duncan’s nonlinear strength criterion. The reliability index for slope stability, based on Bishop’s simplified method, is estimated by the first-order, second-moment method. Expressions of partial derivatives of the limit state function and an iterative process for determination of the reliability index are presented in this paper. The proposed algorithm was coded into a computer program named SCU-SLIDE. The accuracy of the reliability approach was verified by comparison of the program outputs with Monte Carlo simulation results, and influences of variation in the mean values, coefficients of variation and probability distributions of nonlinear strength parameters on slope reliability were examined. The SCU-SLIDE program was used to study the slope stability of the Shuang Jiang Kou dam in China, which, when complete, will have a maximum height of 314 m. Some conclusions drawn from the results of this study are presented in this paper.

## 2. Deterministic analysis of slope stability of rockfill dams

### 2.1. Bishop’s simplified method

Bishop’s simplified method [19] was one of the earliest practical approaches to estimating the stability of slopes that was based on the method of slices. Bishop’s simplified method considers normal interslice forces but ignores interslice shear forces and satisfies overall moment equilibrium but not overall horizontal force equilibrium. The forces considered in Bishop’s simplified method are shown in Fig. 1. The good precision of Bishop’s simplified method has been demonstrated by comparison with rigorous methods

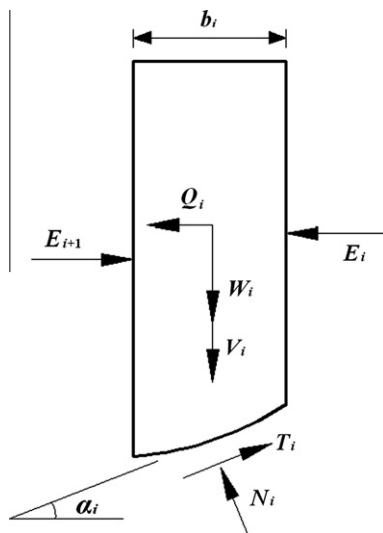


Fig. 1. Forces considered in Bishop’s simplified method of slices.

such as the Morgenstern–Price method [20]. The safety factor given by Bishop’s simplified method is as follows:

$$F_s = \frac{\sum \{[(W + V) \sec \alpha - ub \sec \alpha] \tan \varphi' + c' b \sec \alpha\} [1 / (1 + \tan \alpha \tan \varphi' / F_s)]}{\sum [(W + V) \sin \alpha + M_c / R]} \quad (1)$$

where  $F_s$  is the safety factor;  $W$  is the weight of the slice;  $V$  is the vertical seismic inertia force;  $u$  is the pore water pressure at the base of the slice;  $\alpha$  is the inclination angle of the slice base to the horizontal;  $b$  is the width of the slice;  $c'$  and  $\varphi'$  are, respectively, the effective cohesion and friction angle of the soil (for coarse-grained soil, the cohesion is ignored and the friction angle is about a function of the stress state);  $M_c$  is the moment about the center of the failure arc due to the horizontal seismic inertia force; and  $R$  is the radius of the failure arc.

### 2.2. Nonlinear shear criteria for rockfill

A number of nonlinear shear criteria have been proposed for use in describing the nonlinear characteristics of the shear strength of coarse-grained soils, such as rockfills, gravels and sands, over the last three decades. Some of the latest representative publications include Xu et al. [21], Soroush and Jannatiaghdam [22], Frossard et al. [23], Araei et al. [24] and Shi et al. [25], among others.

According to the Chinese design specifications for rolled earth-rock fill dams (DL/T 5395-2007) [26], it is assumed that the effective friction angle of coarse-grained soil varies with the confining pressure according to the following expression [27]:

$$\varphi' = \varphi_0 - \Delta\varphi \lg \left( \frac{\sigma_3}{P_a} \right) \quad (2)$$

where  $\sigma_3$  is the minor principal stress,  $P_a$  is the atmospheric pressure,  $\varphi_0$  is the effective friction angle under  $1.0 P_a$  and  $\Delta\varphi$  is the reduction in  $\varphi_0$  corresponding to an increase in  $\sigma_3$  during a logarithmic cycle.

## 3. Reliability approach

### 3.1. First-order second-moment method (FOSM)

Before performing structural reliability analysis, the limit state function  $g(X)$  (where  $X$  is the vector of the input stochastic parameters) should be defined to identify the failure and safety state of the structure. In general,  $g(X) > 0$  indicates a safe state and  $g(X) < 0$  indicates a failure state, while  $g(X) = 0$  is the limit state surface.

If the limit state function is linear and the  $X$  variables are normally distributed, the reliability index  $\beta$  is defined as follows:

$$\beta = \frac{\mu_g}{\sigma_g} \quad (3)$$

where  $\mu_g$  is the mean value of the limit state function and  $\sigma_g$  is the standard deviation of the limit state function.

The corresponding probability of failure can be evaluated as follows:

$$P_f = \Phi(-\beta) \quad (4)$$

where  $\Phi(\bullet)$  is the standard normal cumulative distribution function (CDF).

The nonlinear limit state function is first approximated by a first-order polynomial using Taylor’s series expansion with the maximum probabilistic point (MPP),  $\mathbf{x}^*$ , as the expanding point [28]. The MPP is a point that defines the minimum distance (the reliability index  $\beta$ ) from the origin to the limit state surface in a

coordinate system of an independent, standardized normal vector [29]. The mean value of the limit state function is as follows:

$$\mu_g = g(x_1^*, x_2^*, \dots, x_n^*) + \sum_{i=1}^n \frac{\partial g}{\partial X_i} \Big|_{x_i^*} (\mu_{X_i} - x_i^*) \quad (5)$$

Because the MPP is located at the limit state surface, the first term of Eq. (5) is equal to zero. Eq. (5) reduces to the following equation:

$$\mu_g = \sum_{i=1}^n \frac{\partial g}{\partial X_i} \Big|_{x_i^*} (\mu_{X_i} - x_i^*) \quad (6)$$

The standard deviation of the limit state function is as follows:

$$\sigma_g = \left( \sum_{i=1}^n \sum_{j=1}^n \rho_{X_i, X_j} \frac{\partial g}{\partial X_i} \Big|_{x_i^*} \frac{\partial g}{\partial X_j} \Big|_{x_j^*} \sigma_{X_i} \sigma_{X_j} \right)^{1/2} \quad (7)$$

where  $\mu_{X_i}$  is the mean value of variable  $X_i$ ,  $\sigma_{X_i}$  is the standard deviation of variable  $X_i$ ,  $\sigma_{X_j}$  is the standard deviation of variable  $X_j$  and  $\rho_{X_i, X_j}$  is the correlation coefficient between variable  $X_i$  and variable  $X_j$ .

Eq. (7) can be written as follows:

$$\sigma_g = \sum_{i=1}^n \alpha_i \frac{\partial g}{\partial X_i} \Big|_{x_i^*} \sigma_{X_i} \quad (8)$$

where

$$\alpha_i = \frac{\sum_{j=1}^n \rho_{X_i, X_j} \frac{\partial g}{\partial X_j} \Big|_{x_j^*} \sigma_{X_j}}{\left( \sum_{i=1}^n \sum_{j=1}^n \rho_{X_i, X_j} \frac{\partial g}{\partial X_i} \Big|_{x_i^*} \frac{\partial g}{\partial X_j} \Big|_{x_j^*} \sigma_{X_i} \sigma_{X_j} \right)^{1/2}} \quad (9)$$

Substituting Eqs. (6) and (8) into Eq. (3) and rearranging the terms, the following equation can be obtained:

$$\sum_{i=1}^n \frac{\partial g}{\partial X_i} \Big|_{x_i^*} (\mu_{X_i} - x_i^* - \beta \alpha_i \sigma_{X_i}) = 0 \quad (10)$$

The above equation is independent of the form of the limit state function,  $g(X)$ , so the sum of the terms in the parentheses in Eq. (10) is zero and the expression for the MPP,  $\mathbf{x}^*$ , can be found as follows:

$$x_i^* = \mu_{X_i} - \beta \alpha_i \sigma_{X_i} \quad (11)$$

Because the reliability index  $\beta$  is unknown until the MPP have been determined, Eq. (11) needs to be solved by iteration. The iterative process is as follows:

- Assume an initial reliability index  $\beta(0)$  and an initial MPP  $\mathbf{x}^*(0)$ .
- Compute equivalent normal distributions for the non-normal random variables at  $\mathbf{x}^*$  using the Rackwitz–Fiessler algorithm [28]. The equivalent normal parameters can be calculated as follows:

$$\sigma_N = \frac{\phi[\Phi^{-1}(F_X(\mathbf{x}^*))]}{f_X(\mathbf{x}^*)} \quad (12)$$

$$\mu_N = \mathbf{x}^* - \Phi^{-1}[F_X(\mathbf{x}^*)] \sigma_N \quad (13)$$

where  $\sigma_N$  and  $\mu_N$  are the mean and standard deviation of the equivalent normal variable,  $\phi(\bullet)$  is the standard normal probability density function (PDF),  $\Phi^{-1}(\bullet)$  is the inverse standard normal CDF,  $F_X(\bullet)$  is the CDF of the original random variable, and  $f_X(\bullet)$  is the PDF of the original random variable.

- Compute a new reliability index using the Newton–Raphson method:

$$\beta(j+1) = \beta(j) - \frac{g(\mathbf{x}_1^*(j), \mathbf{x}_2^*(j), \dots, \mathbf{x}_n^*(j))}{\sum_{i=1}^n \frac{\partial g}{\partial X_i} \Big|_{x_i^*(j)} \alpha_i \sigma_N} \quad (j = 0, 1, \dots) \quad (14)$$

- A new MPP is calculated as follows:

$$x_i^*(j+1) = \mu_N - \beta(j+1) \alpha_i \sigma_N \quad (j = 0, 1, \dots) \quad (15)$$

- Repeat steps (b) to (d) until the  $\beta$  and MPP values converge.

### 3.2. Limit state function of slope stability and the partial derivatives of the limit state function

By setting  $F_s = 1$  in Eq. (1) and rearranging the terms, the limit state function of slope stability is formulated, using Bishop's simplified method as the stability model, as follows:

$$g(X) = \sum \{[(W+V) \sec \alpha - ub \sec \alpha] \tan \varphi' + c' b \sec \alpha\} [1/(1 + \tan \alpha \tan \varphi')] - \sum [(W+V) \sin \alpha + M_c/R] \quad (16)$$

Although the limit state function of slope stability is generally expressed as follows:

$$g(X) = F_s - 1 \quad (17)$$

Eq. (16) is easier to use for evaluating partial derivatives and provides the same reliability results as Eq. (17).

Here, only the soil strength parameters are considered random variables. The derivatives of the limit state function with respect to the linear strength parameters  $c'$  and  $\varphi'$  are expressed as follows:

$$\frac{\partial g}{\partial c'} = \sum \frac{b}{\cos \alpha + \sin \alpha \tan \varphi'} \quad (18)$$

$$\frac{\partial g}{\partial \varphi'} = \sum \frac{(W \pm V - ub) \cos \alpha - c' b \sin \alpha}{(\cos \alpha \cos \varphi' + \sin \alpha \sin \varphi')^2} \quad (19)$$

The derivatives of the limit state function with respect to the non-linear strength parameters  $\varphi_0$  and  $\Delta\varphi$  are expressed as follows:

$$\frac{\partial g}{\partial \varphi_0} = \frac{\partial g}{\partial \varphi'} \frac{\partial \varphi'}{\partial \varphi_0} = \sum \frac{(W \pm V - ub) \cos \alpha}{(\cos \alpha \cos \varphi' + \sin \alpha \sin \varphi')^2} \quad (20)$$

$$\begin{aligned} \frac{\partial g}{\partial \Delta\varphi} &= \frac{\partial g}{\partial \varphi'} \frac{\partial \varphi'}{\partial \Delta\varphi} \\ &= \sum \frac{(W \pm V - ub) \cos \alpha}{(\cos \alpha \cos \varphi' + \sin \alpha \sin \varphi')^2} \left( -\lg \left( \frac{\sigma_3}{p_a} \right) \right) \end{aligned} \quad (21)$$

and  $\sigma_3$  is calculated as follows [30]:

$$\sigma_3 = \sigma_n (\sec^2 \varphi' - \tan \varphi' \sec \varphi') \quad (22)$$

where  $\sigma_n$  is the stress normal to the failure arc. According to Bishop's simplified method,  $\sigma_n$  is written as follows:

$$\sigma_n = \frac{(W \pm V)}{(b + b \tan \varphi' \tan \alpha)} - u \quad (23)$$

For a homogeneous dam, the symbol  $\sum$  in Eqs. (18)–(21) denotes the sum of all the slices. When multiple of soil types are involved in a dam, the symbol  $\sum$  denotes the sum of the slices of the same soil type.

### 3.3. Verification of the reliability approach

The reliability approach described in this paper was implemented in a computer program, SCU-SLIDE, which was developed in Visual Basic. The reliability indices of a homogenous rockfill embankment obtained from SCU-SLIDE were compared with the output from Monte Carlo simulations. To verify that Eqs. (16) and (17) provide the same reliability results, the limit state function was formulated based on Eq. (17) in the Monte Carlo method.

The rockfill embankment considered in the simulation was a fictitious structure that was assumed to be filled with hard rocks. The height of the embankment was 200 m, the crest width was 10 m, the slope was 1:1.4, and the bulk unit weight of the rockfill

**Table 1**  
The minimum reliability indices of the dam slope for different combinations of  $\varphi_0$  and  $\rho$ .

Mean of $\varphi_0$	Correlation coefficient $\rho$ between $\varphi_0$ and $\Delta\varphi$	$\beta_{\min}$ obtained from the SCU-SLIDE computer program	$\beta_{\min}$ obtained from the Monte Carlo method
53°	0	4.4699	4.4526
52°	0	4.2466	4.2051
51°	0	4.0154	3.9759
50°	0	3.7758	3.7399
49°	0	3.5273	3.4972
48°	0	3.2694	3.2484
48°	0.2	3.6029	3.5682
48°	0.4	4.0447	4.0600
48°	0.6	4.3712	4.4048
48°	0.8	4.4941	4.5318
48°	1.0	4.6939	4.6828

was 22.0 kN/m<sup>3</sup>. According to data on hard rocks from some hydraulic power projects in China, typical coefficients of variation of the nonlinear strength parameters  $\varphi_0$  and  $\Delta\varphi$  are approximately 0.06 and 0.15, respectively; the mean of  $\Delta\varphi$  is approximately 10°, and the mean of  $\varphi_0$  is approximately 53°;  $\varphi_0$  is normally distributed, and  $\Delta\varphi$  is log-normally distributed. The calculated correlation coefficients between  $\varphi_0$  and  $\Delta\varphi$  were greater than zero, which indicates that  $\varphi_0$  and  $\Delta\varphi$  are positively correlated, i.e.,  $\varphi_0$  generally increases as  $\Delta\varphi$  increases and vice versa. To obtain more results for verification, the mean of  $\varphi_0$  was varied from 48° to 53°, and the correlation coefficient  $\rho$  between  $\varphi_0$  and  $\Delta\varphi$  was varied from 0.0 to 1.0.

The minimum reliability indices of slope stability for different combinations of  $\varphi_0$  and  $\rho$  were determined by the computer program and are summarized in Table 1, along with the reliability indices calculated by Monte Carlo simulations.

The reliability indices computed by the computer program are very close to those calculated by the Monte Carlo method, which indicates that the proposed reliability approach has good precision. Furthermore, the results and comparisons show that the limit state function of slope stability can be formulated by either Eq. (16) or Eq. (17).

**4. Sensitivity of slope reliability to statistical parameters of  $\varphi_0$  and  $\Delta\varphi$**

A sensitivity analysis was conducted based on the parameters of the same fictitious rockfill embankment. The statistical parameters of  $\varphi_0$  and  $\Delta\varphi$  can be modified to evaluate their impact on the results of slope reliability analyses.

**4.1. Influence of correlation between  $\varphi_0$  and  $\Delta\varphi$  on slope reliability**

The results of an evaluation of the effect of the correlation coefficient between  $\varphi_0$  and  $\Delta\varphi$  on slope reliability are illustrated in Table 1 and Fig. 2. The reliability index increases with the coefficient of correlation  $\rho$ , while the critical slip surface moves towards the slope face, as shown in Fig. 2.

**4.2. Influence of mean values of  $\varphi_0$  and  $\Delta\varphi$  on slope reliability**

As shown in Figs. 3 and 4, the reliability index increases linearly with the mean value of  $\varphi_0$  and decreases linearly with the mean value of  $\Delta\varphi$ , for all probability distribution types of  $\varphi_0$  and  $\Delta\varphi$ . N–N shows that  $\varphi_0$  and  $\Delta\varphi$  are both normally distributed. LN–N shows that  $\varphi_0$  and  $\Delta\varphi$  are log-normally and normally distributed, respectively. LN–LN shows that  $\varphi_0$  and  $\Delta\varphi$  are both log-normally distributed. N–LN shows that  $\varphi_0$  and  $\Delta\varphi$  are normally and log-normally distributed, respectively. According to Eq. (2), high values of the mean value of  $\varphi_0$  increase the expected values of the resisting forces and consequently increase the reliability index; in contrast, high values of the mean value of  $\Delta\varphi$  decrease the expected values of the resisting forces and consequently decrease the reliability index.

**4.3. Influence of coefficient of variation of  $\varphi_0$  and  $\Delta\varphi$  on slope reliability**

As shown in Figs. 5 and 6, the reliability index decreases nonlinearly and rapidly with the coefficient of variation of  $\varphi_0$  and decreases slowly with the coefficient of variation of  $\Delta\varphi$ , for all probability distribution types. High values of the coefficient of variation increase the variance of the resisting forces and consequently decrease the reliability index.

**4.4. Influence of probability distribution types for  $\varphi_0$  and  $\Delta\varphi$  on slope reliability**

As shown in Fig. 3–6, a normal distribution of  $\varphi_0$  yields a lower value for the reliability index than a log-normal distribution, while a change in the probability distribution type for  $\Delta\varphi$  has little influence on the reliability index.

**5. Case study of the Shuang Jiang Kou dam**

The Shuang Jiang Kou dam is a zoned rockfill dam with a central gravelly soil core, located in southwest China on the Da Du river. This dam was chosen as a case study for the reliability analysis method discussed in the previous sections of this paper. Upon completion of its construction, the dam height will be 314 m above the central core foundation and the crest width will be 16 m. The

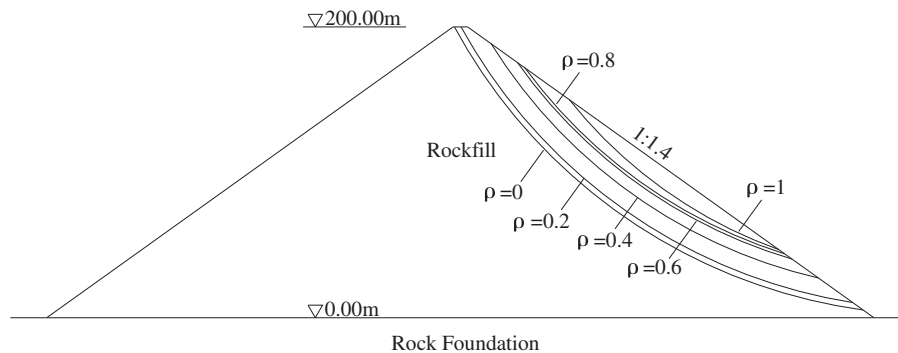


Fig. 2. Variation of critical slip surface with the coefficient of correlation  $\rho$ .

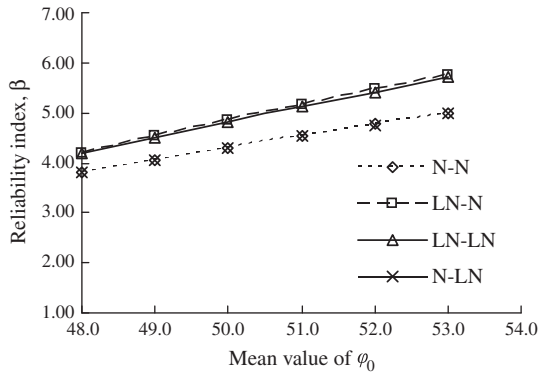


Fig. 3. Variation of the reliability index with the mean value of  $\phi_0$  for different probability distribution types of  $\phi_0$  and  $\Delta\phi$  (the mean value of  $\Delta\phi$  is fixed).

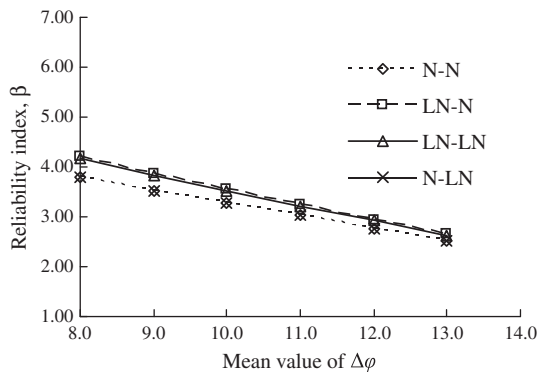


Fig. 4. Variation of the reliability index with the mean value of  $\Delta\phi$  for different probability distribution types of  $\phi_0$  and  $\Delta\phi$  (the mean value of  $\phi_0$  is fixed).

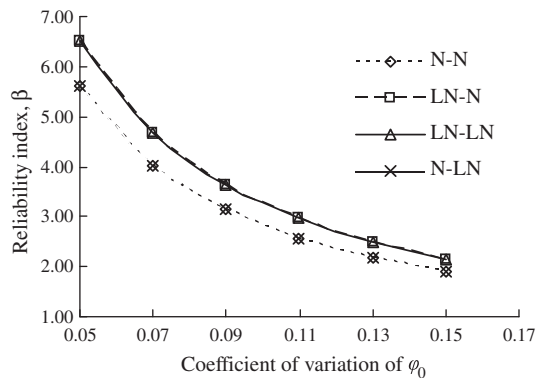


Fig. 5. Variation of the reliability index with the coefficient of variation of  $\phi_0$  for different probability distribution types of  $\phi_0$  and  $\Delta\phi$  (the coefficient of variation of  $\Delta\phi$  is fixed).

reservoir capacity will be 2.732 billion  $m^3$ . The purpose of the dam is to generate power. The annual power generation capacity will be 8.128 billion kW h. A typical cross section of the dam is shown in Fig. 7.

5.1. Statistical data on the shear strength parameters of the soil materials

During the geotechnical investigation of the embankment materials, a large number of samples were taken from borrow areas, and the strength parameters of the soil samples were measured in the laboratory using triaxial compression tests. Based on

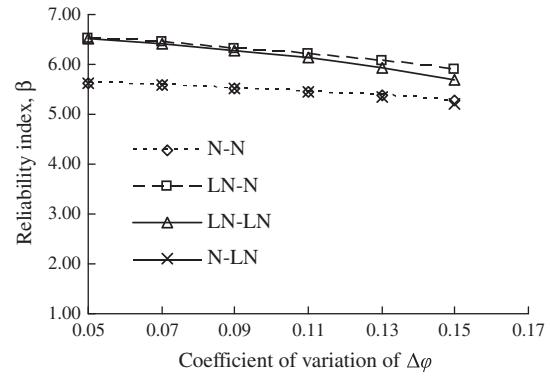


Fig. 6. Variation of the reliability index with the coefficient of variation of  $\Delta\phi$  for different probability distribution types of  $\phi_0$  and  $\Delta\phi$  (the coefficient of variation of  $\phi_0$  is fixed).

the reported results of these tests, the statistical values of the strength parameters for the soils were calculated and are summarized in Table 2. Because of the inadequate number of samples of rock ballast, earth and rock fill material, overburden material and sand, the statistical values of the strength parameters for these materials were mainly based on engineering judgment and experience. In addition, for conservatism in the results of the reliability analysis, the strength parameters  $\phi_0$  and  $\Delta\phi$  were considered to be uncorrelated.

5.2. Results of reliability analysis using the computer program SCU-SLIDE

The computer program SCU-SLIDE was used to calculate the safety factors defined by the mean values of the strength parameters of the soil materials and the reliability indices for the Shuang Jiang Kou dam for various loading conditions. Four loading conditions were considered in the analysis:

- (1) at the end of construction for both the upstream and downstream faces;
- (2) under steady-state seepage at the normal water level for both the upstream and downstream faces;
- (3) under rapid drawdown to the minimum water level for the upstream face; and
- (4) under seismic loading for both the upstream and downstream faces.

During the rapid drawdown process, the rockfill shell is considered to be drained and the core is considered to be undrained; therefore, the phreatic water table migrates with the water level in the rockfill shell and remains unchanged in the core.

Effective stress analysis was used for all the loading cases. The shear strength parameters listed in Table 2 were the consolidated drained effective values. The seismic acceleration considered was 0.2 g, “g” being acceleration due to gravity.

The slip surfaces that might affect the dam were classified into two types: (1) circular slip surfaces that only affect the dam and (2) circular slip surfaces that affect both the dam and the foundation. The critical slip surfaces for each type, based on the minimum safety factor and the minimum reliability index, were determined using a grid-and-radius method.

The minimum safety factors and the minimum reliability indices for the corresponding critical slip surfaces for the end-of-construction loading condition, the steady-state seepage loading condition, the rapid drawdown to minimum water level loading condition and the seismic loading condition are shown in Figs. 8–11, respectively.



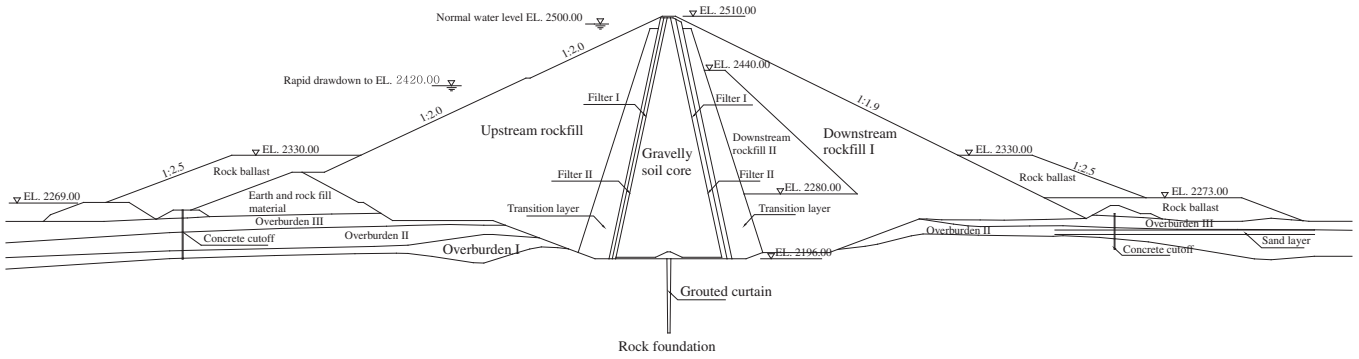


Fig. 7. Main cross-section of the Shuang Jiang Kou dam (material description in Table 2).

Table 2  
Statistical values of the drained shear strength parameters for the soil materials of the Shuang Jiang Kou dam.

Material type	Strength parameter	Probability distribution type	Mean value $\mu$	Standard deviation $\sigma$	Coefficient of variation $V_x$
Downstream rockfill I	$\varphi_0$ (°)	Normal	48.15	2.95	0.06
	$\Delta\varphi$ (°)	Log-normal	6.35	1.41	0.22
Downstream rockfill II	$\varphi_0$ (°)	Normal	42.75	2.26	0.05
	$\Delta\varphi$ (°)	Log-normal	3.59	1.24	0.35
Upstream rockfill	$\varphi_0$ (°)	Normal	42.75	2.26	0.05
	$\Delta\varphi$ (°)	Log-normal	3.59	1.24	0.35
Filter I	$\varphi_0$ (°)	Normal	43.38	2.17	0.05
	$\Delta\varphi$ (°)	Log-normal	3.74	0.77	0.21
Filter II	$\varphi_0$ (°)	Normal	45.83	2.59	0.06
	$\Delta\varphi$ (°)	Log-normal	5.45	2.19	0.40
Transition layer	$\varphi_0$ (°)	Normal	46.11	2.31	0.05
	$\Delta\varphi$ (°)	Log-normal	5.04	1.13	0.22
Gravelly soil	$c$ (kPa)	Normal	89.57	23.79	0.27
	$\varphi$ (°)	Log-normal	34.38	5.92	0.17
Rock ballast	$\varphi$ (°)	Normal	36.49	1.82	0.05
Earth and rock fill material	$\varphi$ (°)	Normal	36.49	1.82	0.05
Overburden III	$\varphi$ (°)	Normal	31.00	4.65	0.15
Overburden II	$\varphi$ (°)	Normal	27.00	4.05	0.15
Overburden I	$\varphi$ (°)	Normal	31.00	4.65	0.15
Sand layer	$\varphi$ (°)	Normal	20.00	3.00	0.15

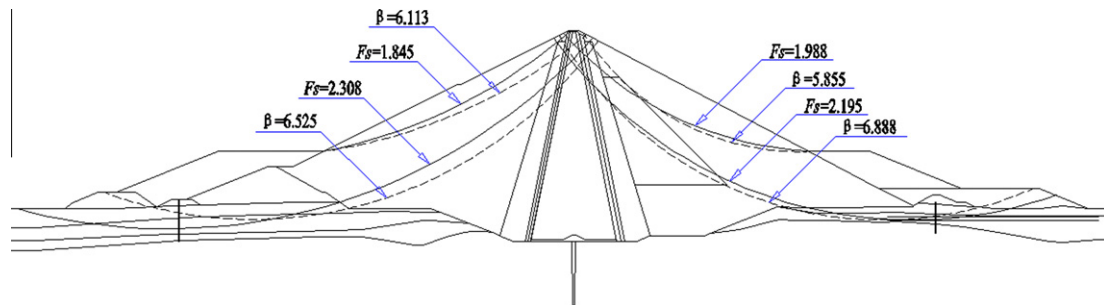


Fig. 8. Critical slip surfaces based on the minimum safety factor and minimum reliability index of the Shuang Jiang Kou dam at the end of construction.

5.3. Discussion of the results

As observed from Figs. 8–11, the critical slip surface based on the minimum safety factor is not the same as the one based on the minimum reliability index, and the zone with a higher value for the safety factor does not necessarily have a higher value for the reliability index. In conventional deterministic analysis, the strength parameters of the soil materials would be considered constant values. However, because of the inherent randomness of soil properties and measurement errors, the strength parameters of

soils are not deterministic; from a probabilistic point of view, they are stochastic variables. Thus, the slip surface with the minimum safety factor is not necessarily the most probable failure arc due to the variability in the shear strength of soils.

The Shuang Jiang Kou dam will be 314 m high and will store a huge volume of water. Its failure would result in serious disasters. Therefore, it is important to assess both the degree of safety and the level of risk of the dam slope. According to the Chinese design specification for rolled earth–rock fill dams (DL/T 5395-2007) [26] and the unified design standard for reliability of hydraulic

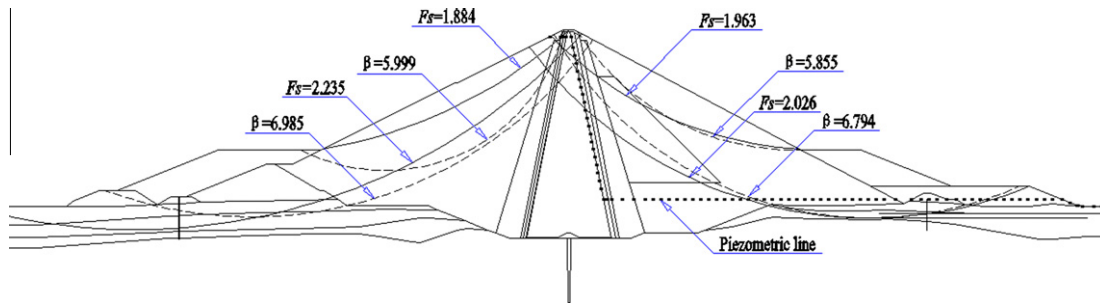


Fig. 9. Critical slip surfaces based on the minimum safety factor and minimum reliability index of the Shuang Jiang Kou dam under steady-state seepage.

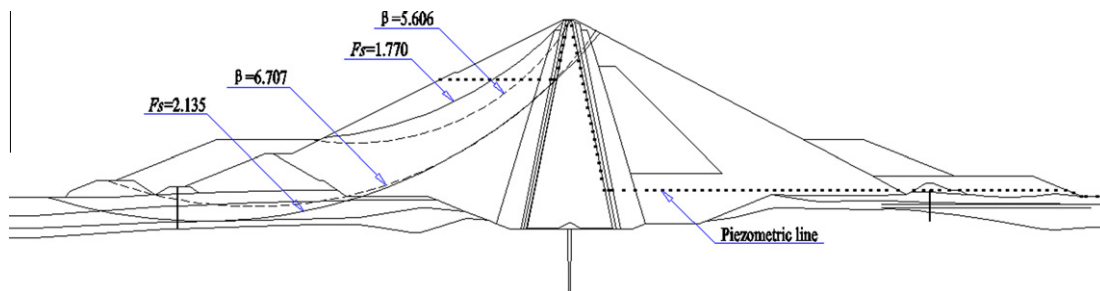


Fig. 10. Critical slip surfaces based on the minimum safety factor and minimum reliability index of the Shuang Jiang Kou dam during rapid drawdown to the minimum water level.

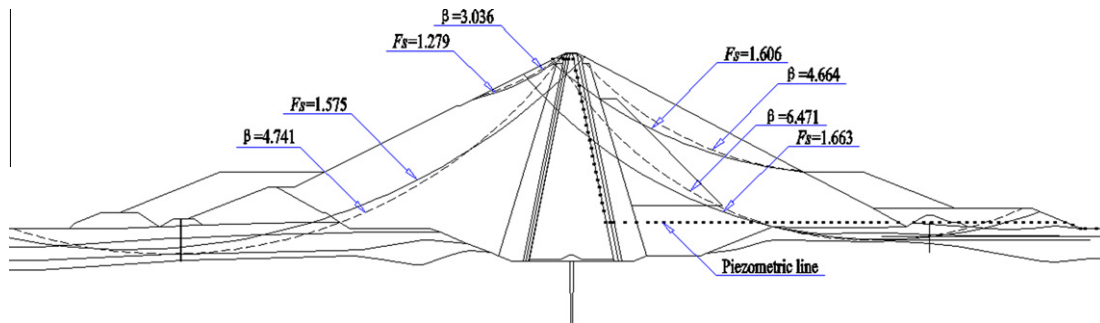


Fig. 11. Critical slip surfaces based on the minimum safety factor and minimum reliability index of the Shuang Jiang Kou dam for seismic loading.

engineering structures (GB 50199-94) [31], any slip surface affecting the dam must have a minimum safety factor of 1.5 under steady-state seepage, a minimum safety factor of 1.3 at the end of construction and under rapid drawdown, and a minimum safety factor of 1.2 for seismic loading. For all these cases, a minimum reliability index of 4.2 is needed.

The results show that the safety factors were higher than the required minimum safety factor in all cases and that the lowest safety factor obtained was 1.279, for seismic loading. Moreover, the safety factors related to the slip surfaces that affect both the dam and the foundation are higher than those related to the slip surfaces that only affect the dam.

Apart from the upstream slope in the seismic loading case, the calculated reliability indices all exceed the required minimum reliability index. The most probable failure arc is located at the upstream face near the normal water level in the seismic loading case. Ideally, the probability of the seismic event considered in the analysis should be taken into consideration, but because the determination of this probability is difficult, it was not considered in the calculation. Thus, the result for the seismic loading case is conservative. Even though the most critical slip surface is superfi-

cial and would not seriously affect the integrity of the structure and even though the slope stability analysis result for the seismic loading case is on the safe side, it is suggested that the region around the slip surface be reinforced.

## 6. Conclusions

The main conclusions of this paper may be summarized as follows:

- (1) Triaxial compression tests reveal that the failure envelopes of rockfills were curved; therefore, nonlinear shear characteristics should be considered in reliability analysis of the slope stability of rockfill embankment dams.
- (2) A reliability-based approach for evaluating the slope stability of high rockfill dams was developed. The proposed algorithm models and analyze the uncertainties associated with the parameters  $\varphi_0$  and  $\Delta\varphi$  of Duncan's nonlinear strength criterion. The proposed algorithm was coded into a computer program and compared to a Monte Carlo simulation for validation.

- (3) Slope reliability is sensitive to the statistical parameters and probability distribution types of  $\varphi_0$  and  $\Delta\varphi$  and to the correlation between  $\varphi_0$  and  $\Delta\varphi$ .
- (4) The safety factors calculated for the Shuang Jiang Kou dam are higher than the required minimum safety factors for all loading conditions considered, including seismic loading. The lowest reliability index for the upstream face, near the normal water level, is below the target value in the case of a seismic event. Because a conservative assumption is made regarding the correlation between  $\varphi_0$  and  $\Delta\varphi$ , the actual reliability is higher.
- (5) The case study demonstrated that the slip surface with the minimum safety factor is not necessarily the most probable one, and a safety factor greater than the target value does not necessarily prevent failure of the slope. Thus, it is beneficial to calculate both the safety factor and the reliability index of the dam slope.
- (6) In this study, only nonlinear shear strength parameters were treated as stochastic variables in the reliability analysis. In fact, there are other random factors that influence the reliability of slope stability, such as the variation of pore pressure and the weights of materials. In addition, the values of the random factors that influence the reliability of slope stability vary over the slip surface, and so stochastic field theory should be applied. Future research will focus on these issues.

## Acknowledgement

Financial support provided by the National Natural Science Foundation of China (No. 51109151) is gratefully acknowledged.

## References

- [1] Leps TM. Review of shearing strength of rockfill. *J Soil Mech Found Div* 1970;96(SM4):1159–70.
- [2] Charles JA, Watts KS. The influence of confining pressure on the shear strength of compacted rockfill. *Geotechnique* 1980;30(4):353–67.
- [3] Oyanguren Ramírez P, Nicieza González C, Fernándezálvarez MI, Palacios González C. Stability analysis of Llerin rockfill dam: an in situ direct shear test. *Eng Geol* 2008;100:120–30.
- [4] Indraratna B. The effect of normal stress–friction angle relationship on the stability analysis of a rockfill dam. *Geotech Geol Eng* 1994;12(2):113–21.
- [5] Tang XS, Li DQ, Zhou CB, Zhang LM. Improved knowledge-based clustered partitioning and its application to slope reliability analysis. *Comput Geotech* 2012;39(1):34–43.
- [6] Zhang S, Zhang LM, Peng M, Zhang LL, Zhao HF, Chen HX. Assessment of risks of loose landslide deposits formed by the 2008 Wenchuan earthquake. *Nat Hazards Earth Syst Sci* 2012;12:1381–92.
- [7] Zhang J, Tang WH, Zhang LM, Huang HW. Characterising geotechnical model uncertainty by hybrid Markov chain Monte Carlo simulation. *Computer Geotech* 2012;39(1):26–36.
- [8] Raihan Taha Mohd, Mohammad Khajehzadeh, El-Shafie Ahmed. Application of particle swarm optimization in evaluating the reliability of soil slope stability analysis. *Sains Malaysiana* 2012;41(7):847–54.
- [9] Chiu CF, Yan WM, Ka-Veng Yuen. Reliability analysis of soil–water characteristics curve and its application to slope stability analysis. *Eng Geol* 2012;135:83–91.
- [10] Irigaray C, El Hamdouni R, Jimenez-Peralvarez JD. Spatial stability of slope cuts in rock massifs using GIS technology and probabilistic analysis. *Bull Eng Geol Environ* 2012;71(3):569–78.
- [11] Fisher Brendan R, Eberhardt Erik. Assessment of parameter uncertainty associated with dip slope stability analyses as a means to improve site investigations. *J Geotech Geoenviron Eng* 2012;138(2):166–73.
- [12] Naghadehi Masoud Zare, Jimenez Rafael, KhaloKakaie Reza. A probabilistic systems methodology to analyze the importance of factors affecting the stability of rock slopes. *Eng Geol* 2011;118(3):82–92.
- [13] Srivastava Amit, Babu GL Sivakumar. Total risk rating and stability analysis of embankment dams in the Kachchh Region, Gujarat, India. *Eng Geol* 2010;115(1):68–79.
- [14] Leynaud D, Sultan N. 3-D Slope stability analysis: a probability approach applied to the nice slope (SE France). *Mar Geol* 2010;269(3):89–106.
- [15] Suchomel R, Masin D. Comparison of different probabilistic methods for predicting stability of a slope in spatially variable c-phi soil. *Comput Geotech* 2010;37(1):132–40.
- [16] Wang Yu, Cao Zijun, Au Siu-Kui. Efficient Monte Carlo Simulation of parameter sensitivity in probabilistic slope stability analysis. *Comput Geotech* 2010;37(7):1015–22.
- [17] Chowdhury R, Rab BN. Probabilistic stability assessment of slopes using high dimensional model representation. *Comput Geotech* 2010;37(7):876–84.
- [18] Mbarka S, Baroth J, Ltifi M, Hassis H, Darve F. Reliability analyses of slope stability Homogeneous slope with circular failure. *Eur J Environ Civil Eng* 2010;14(10):1227–57.
- [19] Bishop AW. The use of slip circle in the stability analysis of slopes. *Geotechnique* 1955;5:7–17.
- [20] Morgenstern NR, Price VE. The analysis of the stability of general slip surfaces. *Geotechnique* 1965;15(1):79–93.
- [21] Xu Ming, Song Erxiang, Chen Jinfeng. A large triaxial investigation of the stress–path–dependent behavior of compacted rockfill. *Acta Geotech* 2012;7(3):167–75.
- [22] Soroush A, Jannatiaghdam R. Behavior of rockfill materials in triaxial compression testing. *Int J Civil Eng* 2012;10(2):153–61.
- [23] Frossard E, Hu W, Dano C. Rockfill shear strength evaluation: a rational method based on size effects. *Geotechnique* 2012;62(5):415–27.
- [24] Araei A Aghaei, Soroush A, Rayhani M. Large-scale triaxial testing and numerical modeling of rounded and angular rockfill materials. *Sci Iran Trans A-Civil Eng* 2010;17(3):169–83.
- [25] Shi Wei-cheng, Zhu Jun-gao, Chiu Chung-fai. Strength and deformation behaviour of coarse-grained soil by true triaxial tests. *J Central South Univ Technol* 2010;17(5):1095–102.
- [26] National Development and Reform Commission, PRC. Chinese design specifications for rolled earth–rock fill dams (industry standard no. DL/T 5395–2007). Beijing: China Electric Power Press; 2008.
- [27] Duncan JM, Byrne PM, Wong KS. Strength, stress–strain and bulk modulus parameters for finite element analysis of stress and movements in soil masses (research report no. VCB/GT/78–02). Berkeley: University of California; 1978.
- [28] Rackwitz R, Fiessler B. Structural reliability under combined load sequences. *J Comput Struct* 1978;9:489–94.
- [29] Ang AHS, Tang WH. Probability concepts in engineering planning and design, Volume II: Decision, risk and reliability. New York: John Wiley & Sons; 1984.
- [30] Chen ZY. Slope stability analysis using nonlinear strength parameters. *Water Power* 1990;9:9–13.
- [31] The Ministry of Water Resources of the PRC. Unified design standard for reliability of hydraulic engineering structures (national standard no. GB 50199–94). Beijing: China Planning Press; 1994.